Analysis of the Rare Decay $B_s \to f_2' \mu^+ \mu^-$

Intern Documentation

Daniel Berninghoff

17. September 2014

A search for the decay $B_s \to f_2' \mu^+ \mu^-$, where $J/\psi \to \mu^+ \mu^-$, was performed using data, corresponding to an integrated luminosity $\mathcal{L} = 3.0\,\mathrm{fb}^{-1}$, collected with the LHCb detector. This decay is highly suppressed within the Standard Model and is therefore sensitive to New Physics.
Moreover, an analysis for the already observed decay $B_s \to f_2' J/\psi$ is performed which is used as a normalisation channel [1].

Inhaltsverzeichnis

1 Analysis Strategy

We will calculate the branching ratio $\mathcal{B}(B_s \to f_2'\mu^+\mu^-)$, which is referred to as the non-resonant channel, with help of the so called resonant channel $B_s \to f_2' J/\psi$. Using this, the branching ratio can be obtained from

$$\mathcal{B}(\text{non-resonant}) = \frac{\mathcal{B}(\text{resonant})\epsilon_{\text{res}}}{N_{\text{obs, res}}} \frac{N_{\text{obs, non-res}}}{\epsilon_{\text{non-res}}} \,. \tag{1}$$

where N_{obs} are the observed events after applying the selection, which will be explained later, and ϵ the efficiency of this selection.

2 Available Data and Simulations

The data used in this analysis was collected 2011 and 2012 by the LHCb detector. The center of mass energy of the proton-proton collisions was $\sqrt{s} = 7\,\text{TeV}$ (2011) and $\sqrt{s} = 8\,\text{TeV}$ (2012). Moreover, a Monte Carlo simulation (MC) for the decay $B_s \to f_2'\mu^+\mu^-$ with $f_2' \to K^+K^-$ is available to investigate the properties of the signal events.

3 Preselection

To already get rid of a good amount of background, we will apply a rough preselection to the already stripped data. The used preselection is shown in table 1. We apply the cuts

Tab. 1: Preselection that is applied to the stripped data

Preselection variable	Requirement
Kaon DLL$(K-\pi)$	> -3
Kaon DLL$(K-p)$	> -3
Dikaon mass	$1300 < m(KK) < 1800$

on the RICH ID variables to remove potential protons and pions which were misidentified as kaons. The figures 1 and 2 show that, using these cut values, not many signal events are affected by this. We only want to look at the resonance $f_2'(1525)$ with a mass of $(1525 \pm 5)\,\text{MeV/c}^2$ [2] which is why we cut on the combined mass of the two kaons. The cut values were chosen by looking at truthmatched MC (see figure 3).

The figures 4a and 4b show the combined B_s mass distribution before (that means after stripping) and after the preselection. Moreover, figures 5a-7b show the mass distributions when you correct the misidentification mentioned above and correct the masses of the

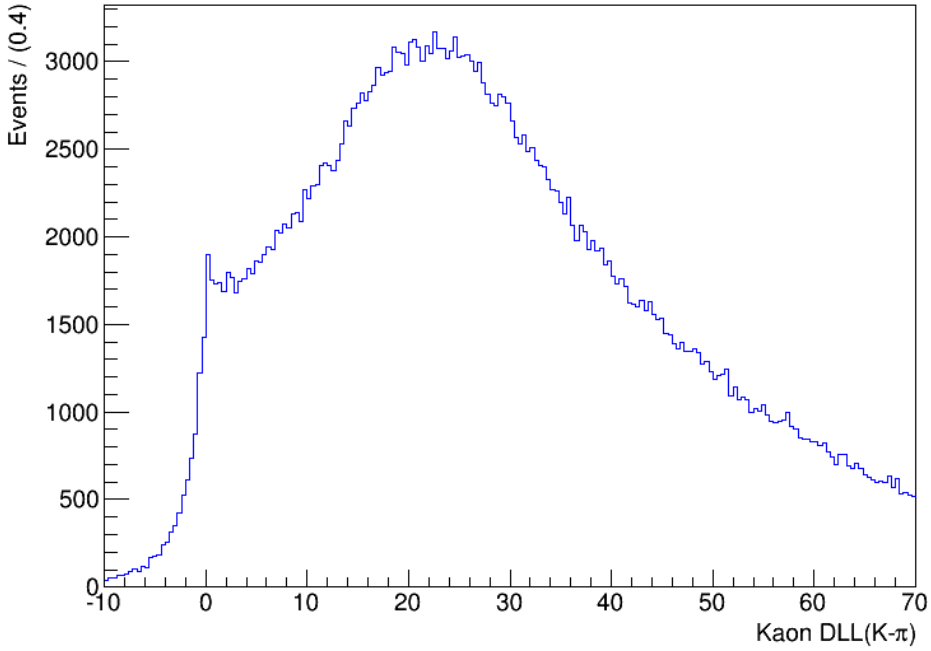

Abb. 1: Kaon DLL($K - \pi$) distribution of truthmatched MC after stripping

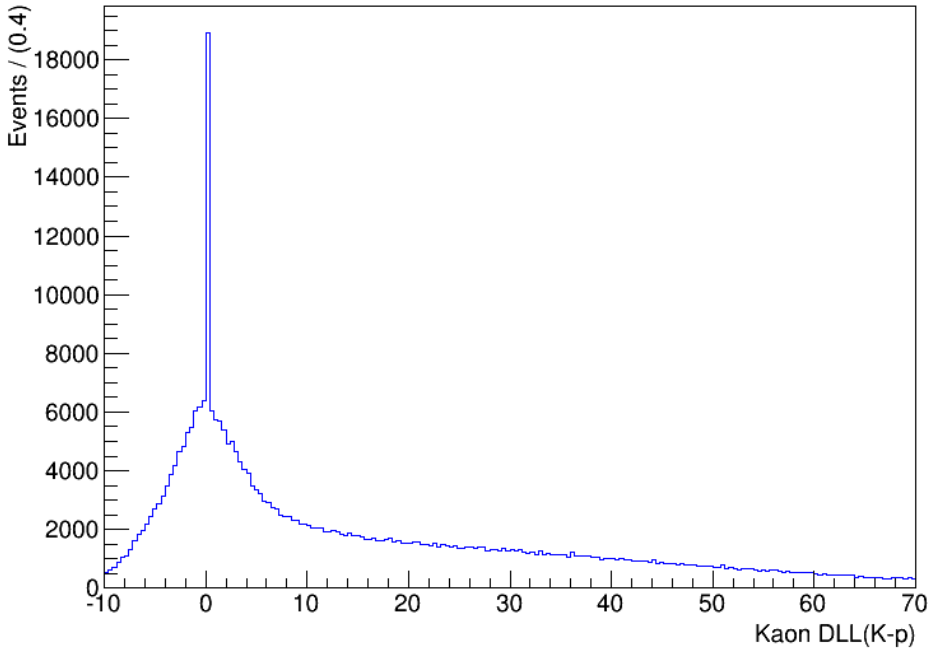

Abb. 2: Kaon DLL($K - p$) distribution of truthmatched MC after stripping

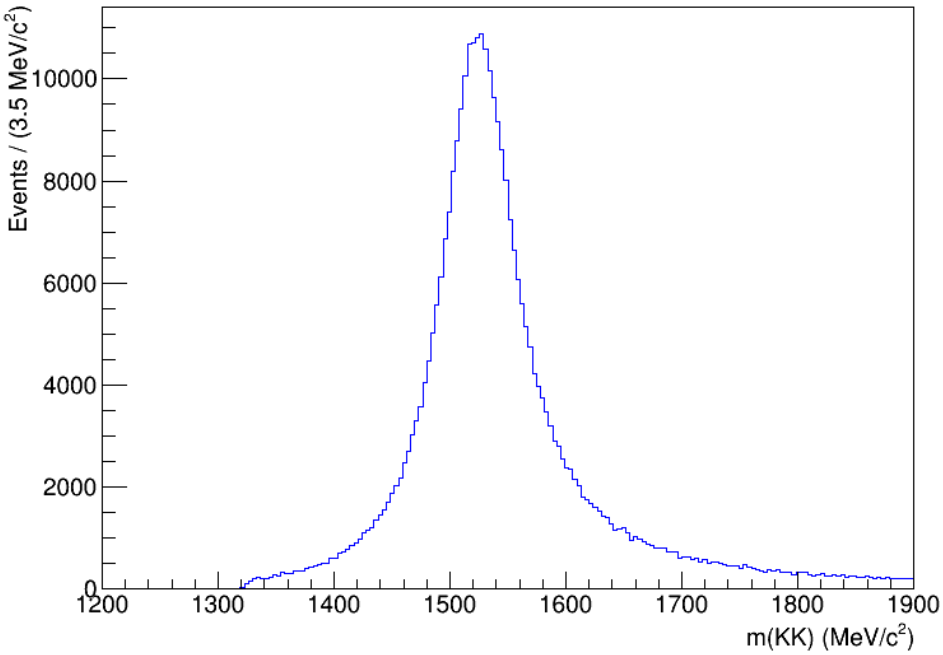

Abb. 3: Combined dikaon mass of truthmatched MC after stripping

kaons to either the pion or the proton mass. When looking at the combined kaon-proton mass, the peak at $\sim 900\,\mathrm{MeV/c^2}$ could belong to the decays $B \to J/\psi K^*$ and $B \to K^*\mu\mu$ where $K^* \to K\pi$ and is still visible after applying our preselection. We also see multiple peaks and bumps in the combined kaon-pion mass distribution. One of them possibly belong to the decay $\Lambda_b \to \Lambda(1520)\mu\mu$. These peaking backgrounds have to be considered in the later stages of the analysis.

4 Trigger Requirements

In terms of the trigger, we use the trigger requirements shown in table 2

5 BDT Training

To further separate background and signal, we use a Multivariate Data Analysis in form of a Boosted Decision Tree (BDT). Therefore TMVA in the version 4.2.0 is used. For the BDT training we use truthmatched MC as signal sample and a B_s mass sideband (from data) as background sample. To both samples we apply the preselection and also the trigger requirements mentioned above. Furthermore, because we mostly want to be

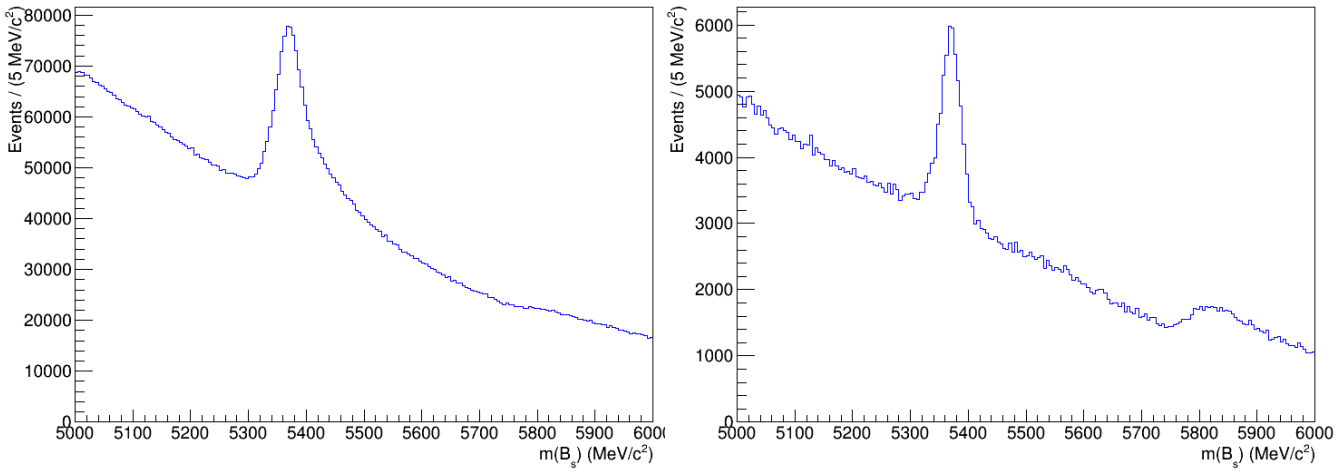

(a) before preselection **(b)** after preselection

Abb. 4: Distribution of the combined B_s mass

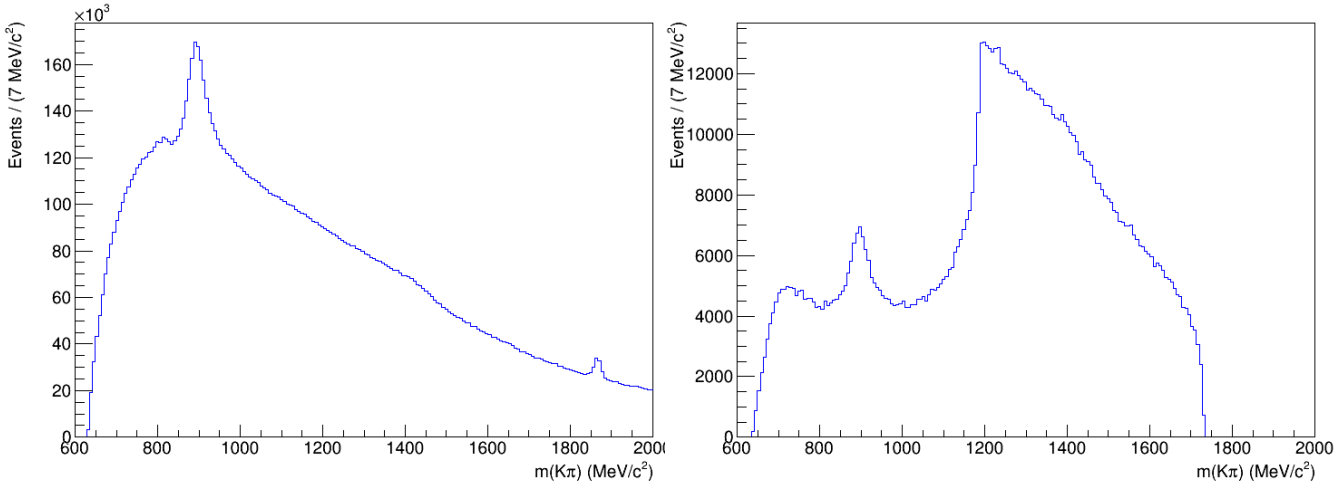

(a) before preselection **(b)** after preselection

Abb. 5: Distribution of combined kaon and pion mass

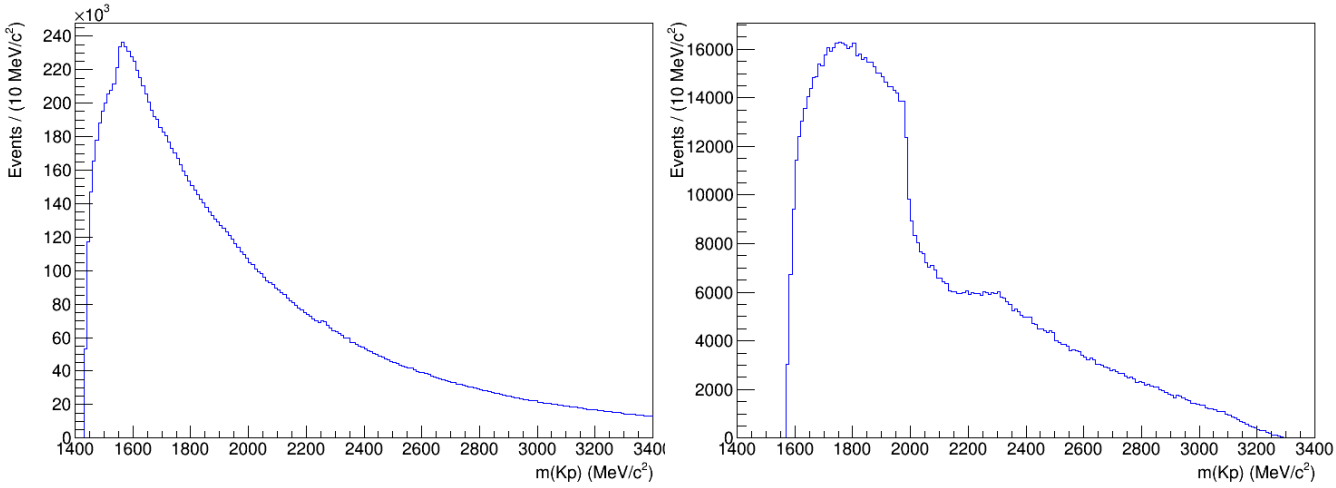

(a) before preselection **(b)** after preselection

Abb. 6: Distribution of combined kaon and proton mass

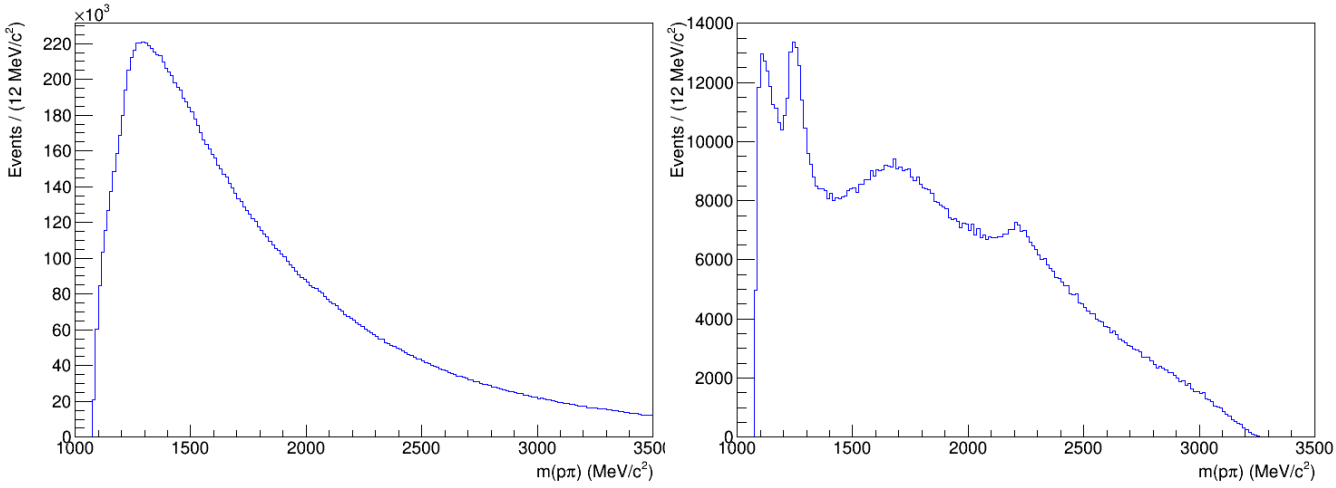

(a) before preselection **(b)** after preselection

Abb. 7: Distribution of combined proton and pion mass

Tab. 2: Used Trigger Requirements

Trigger	Requirement
L0	B0_L0MuonDecision_TOS
	B0_L0DiMuonDecision_TOS
Hlt1	B0_Hlt1TrackAllL0Decision_TOS
	B0_Hlt1TrackMuonDecision_TOS
	B0_Hlt1DiMuonLowMassDecision_TOS
	B0_Hlt1DiMuonHighMassDecision_TOS
	B0_Hlt1SingleMuonHighPTDecision_TOS
Hlt2	B0_Hlt2(Single,Di)MuonDecision_TOS
	B0_Hlt2DiMuonDetachedDecision_TOS
	B0_Hlt2DiMuonDetachedHeavyDecision_TOS
	B0_Hlt2Topo(2,3,4)BodyBBDTDecision_TOS
	B0_Hlt2TopoMu(2,3,4)BodyBBDTDecision_TOS

Tab. 3: Requirements applied to the samples used for the BDT training

Sample	Description	Cut
Signal	Truthmatched MC	B0_BKGCAT == 20
Background	B_s mass sideband	$5500\,\text{MeV} < m(B_s) < 5700\,\text{MeV}$
Both	Preselection	see table 1
	Trigger	see table 2
	J/ψ VETO	$2828.4\,\text{MeV} < m(\mu\mu) < 3316.6\,\text{MeV}$
	Ψ(2S) VETO	$3535.6\,\text{MeV} < m(\mu\mu) < 3535.6\,\text{MeV}$

sensitive to the rare decay $B_s \to f_2'\mu^+\mu^-$ rather than the resonant decay $B_s \to f_2' J/\psi$, we cut out J/ψ and Ψ(2S) resonances in the combined dimuon mass. Table 3 shows the detailed description of the applied cuts to the two samples.

Figures 8-9 show the used variables for the BDT training and their distributions for the background (red) and signal (blue) sample. Note that we do not use any kinematic variables of the muons to be also sensitive for the resonant channel $B_s \to f_2' J/\psi$. The used training settings are shown in table 4. With these settings we get a good separation between signal and background, while not having problems with potential overtraining (see figure 10).

To find the optimal cut on the BDT response, we use the so called Punzi Figure of Merit

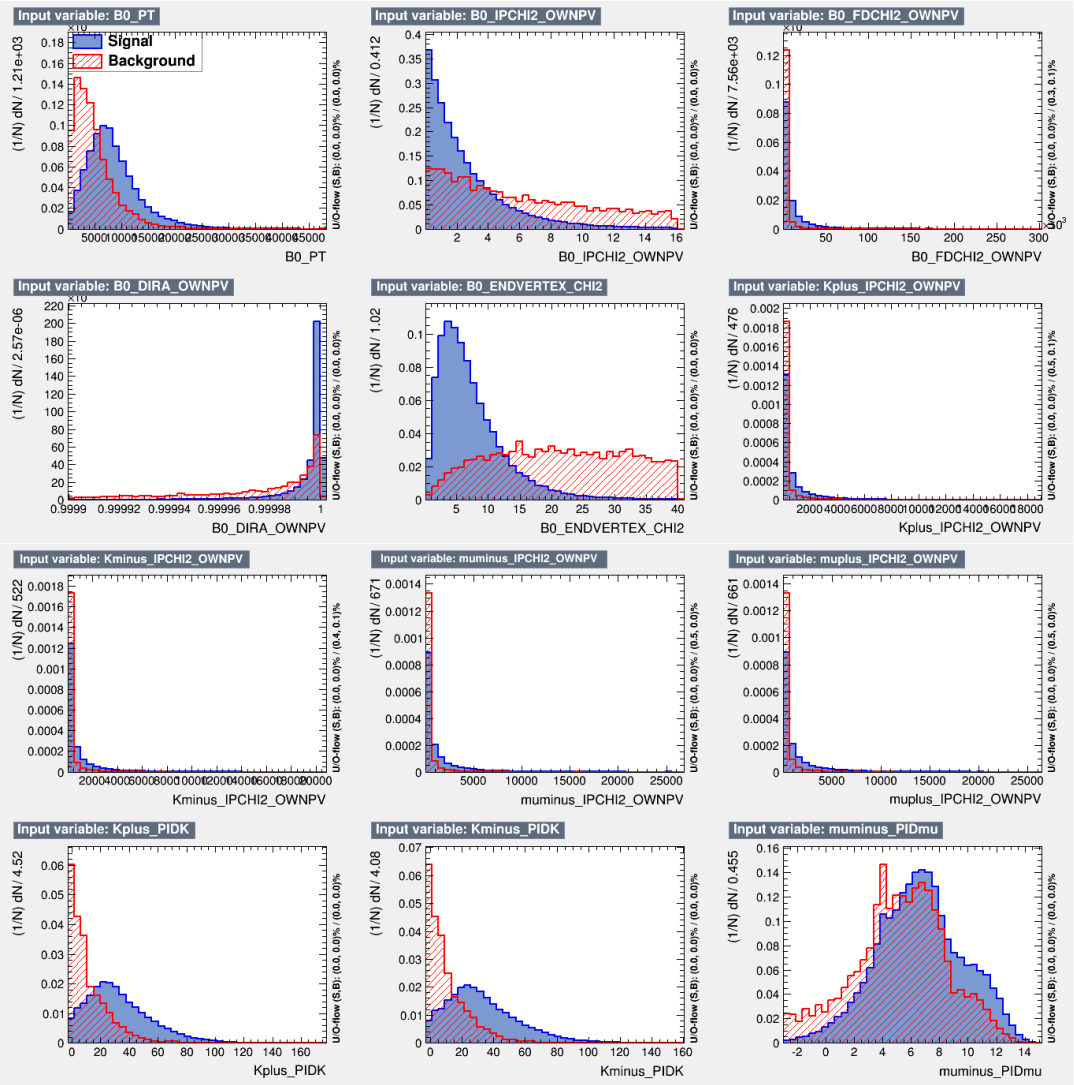

Abb. 8: BDT input variables (1/2). blue: signal, red: background

Tab. 4: BDT training settings

Setting	Value
NTrees	800
MinNodeSize	2.5 %
MaxDepth	2
BoostType	AdaBoost
AdaBoostBeta	0.5
SeparationType	GiniInex
nCuts	150

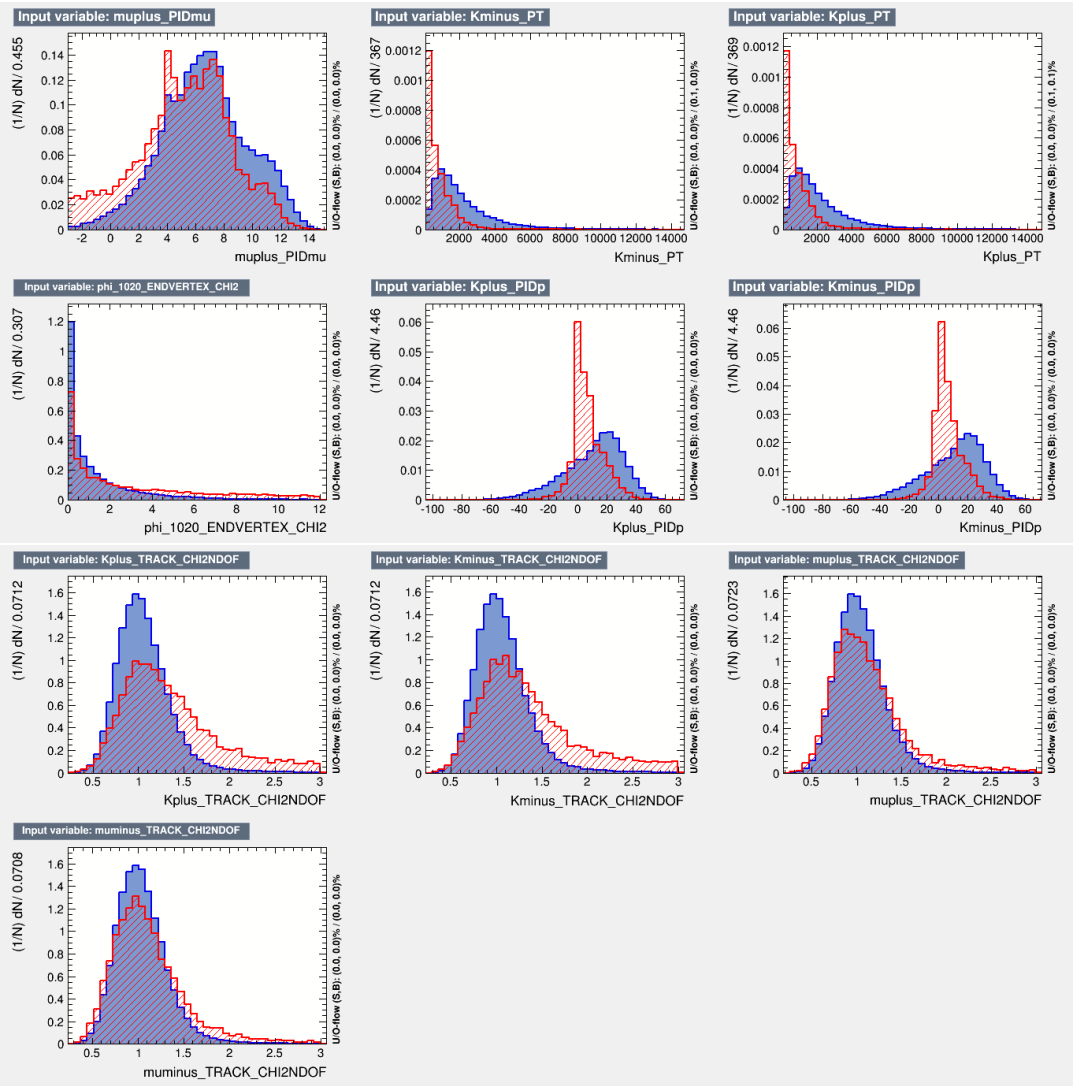

Abb. 9: BDT input variables (2/2). blue: signal, red: background

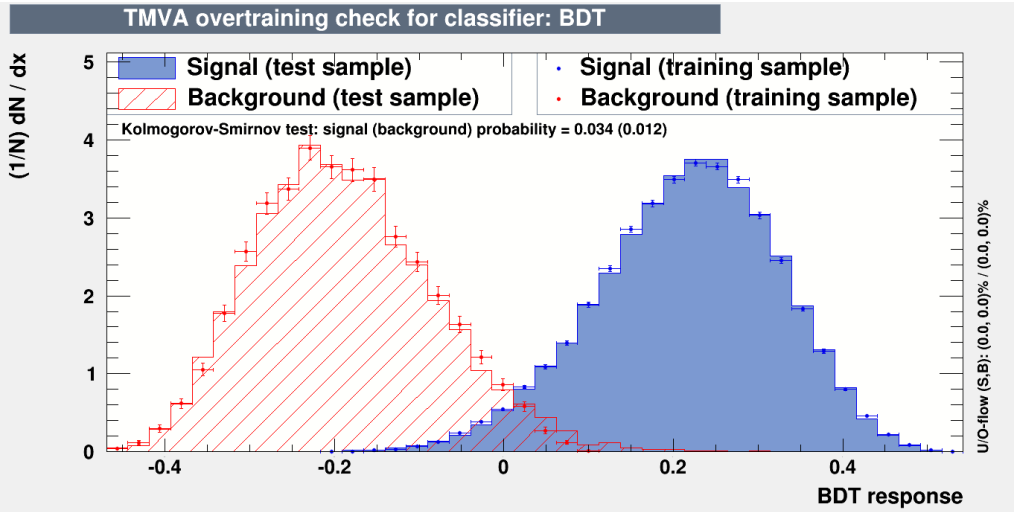

Abb. 10: Overtraining check after training

(FOM)

$$\mathrm{FOM}_{\mathrm{Punzi}} = \frac{\epsilon(c)}{N_\sigma/2 + \sqrt{B(c)}} \tag{2}$$

where ϵ is the signal efficiency when applying the cut c, N_σ is the number of desired standard deviations (we use $N_\sigma = 5$) and B the number of background events in the signal region of $\pm 50\,\mathrm{MeV}$ around the nominal mass of the B_s meson [3].

Therefore it is necessary to know the number of background events before applying the cut on the BDT response. We get an estimate for that by fitting the B_s mass of the background sample with an exponential function and extrapolating it into the signal region (see figure 11). We obtain $B = 9814.5 \pm 201.5$ background events before applying the cut on the BDT response. Maximising the Punzi FOM (2) then yields to a cut at

$$\text{BDT Response} > 0.244909\,. \tag{3}$$

6 Applying the BDT

To check our selection, we will first take a look at the resonant channel $B_s \to f_2' J/\psi$, that we use as control channel. To select this decay we apply the cut listed in table 5. An illustration of that can be also seen in figure 12 where the combined dimuon mass is shown after the stripping.

Figures 13a and 13b show the combined B_s and dikaon mass after applying the complete selection (i.e. stripping, preselection, trigger requirements and BDT cut) to the resonant channel.

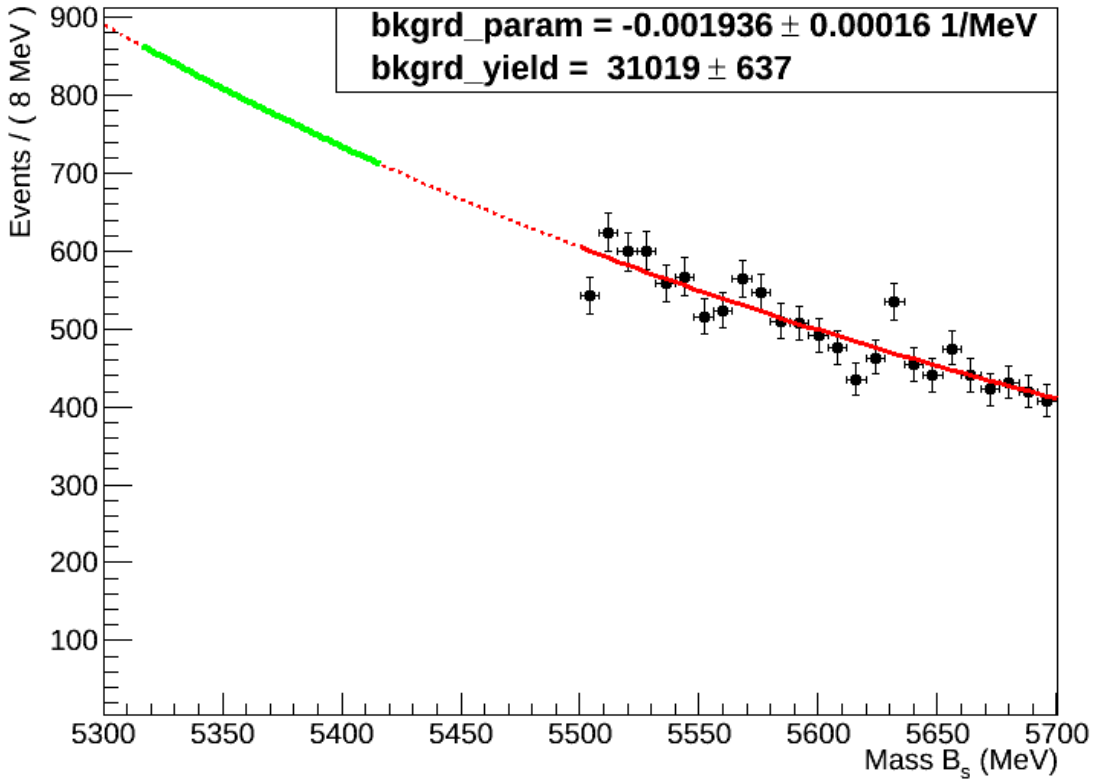

Abb. 11: Fit of the B_s mass of the background sample to get an estimate for the background events in the signal region (green). Red-solid: fit range, red-dashed: extrapolation range

Tab. 5: Cuts to select the decays

Channel	Variable	Value
Resonant	Dimuon mass	$3047\,\text{MeV} < m(\mu\mu) < 3147\,\text{MeV}$
Non-resonant	J/ψ VETO	$2828.4\,\text{MeV} < m(\mu\mu) < 3316.6\,\text{MeV}$
	$\Psi(2S)$ VETO	$3535.6\,\text{MeV} < m(\mu\mu) < 3873.0\,\text{MeV}$

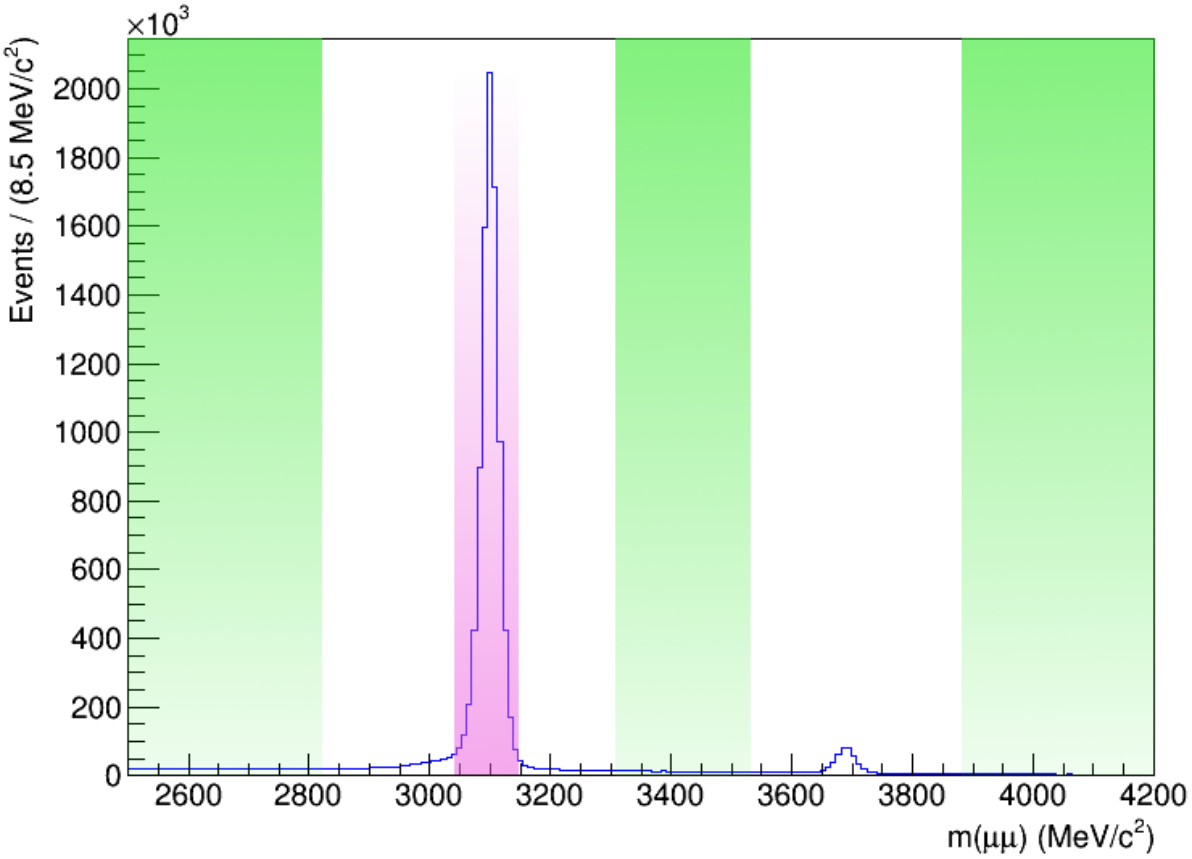

Abb. 12: Distribution of the combined dimuon mass after the stripping. Green: non-resonant channel, violet: resonant channel

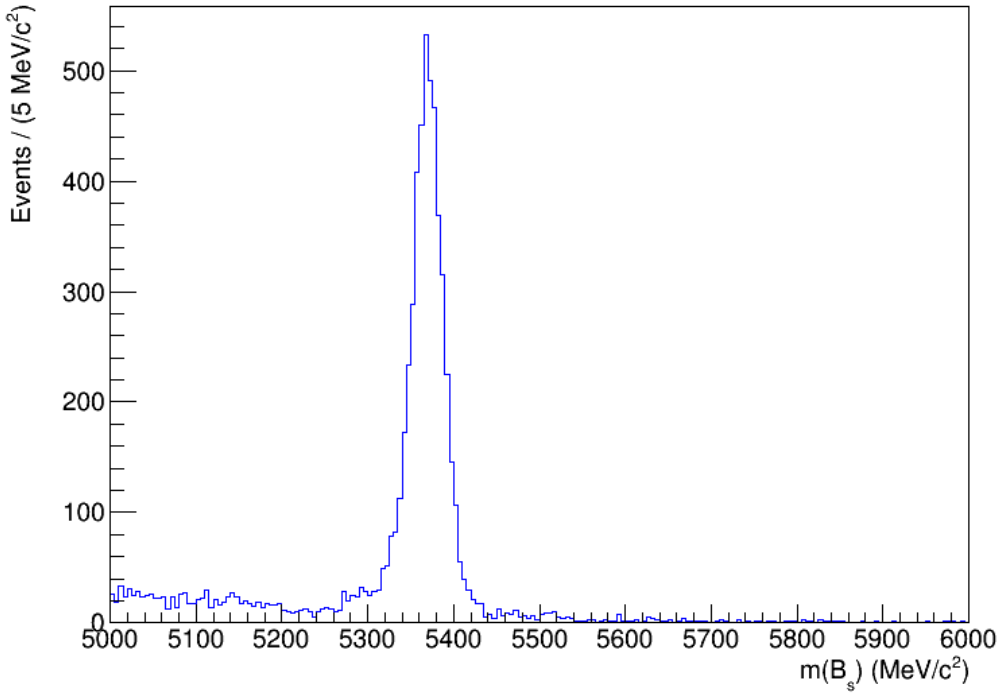

(a) Combined B_s mass

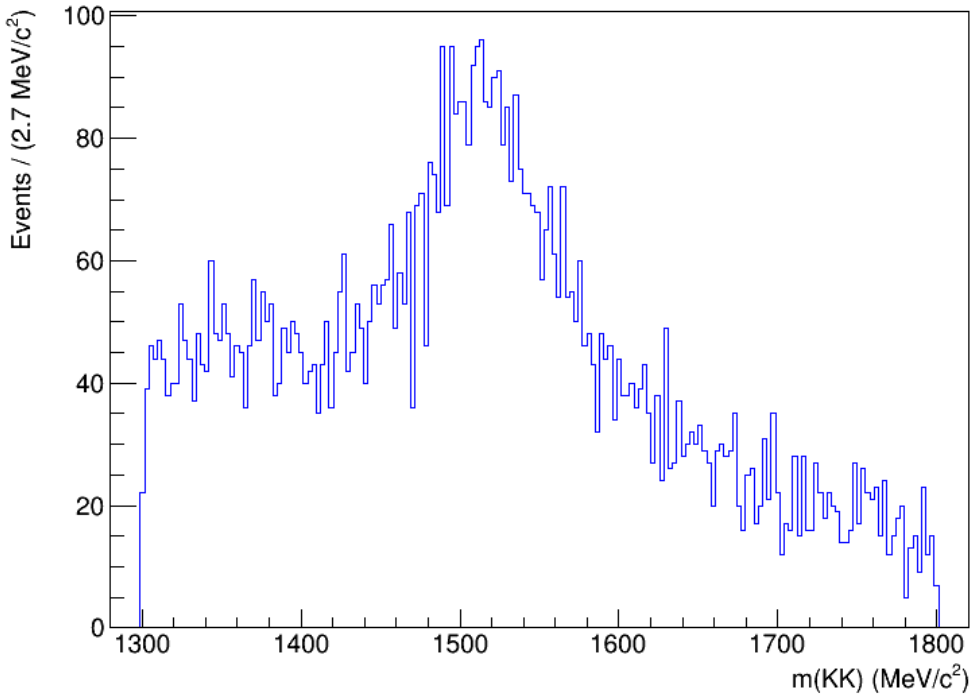

(b) Combined dikaon mass

Abb. 13: Mass distributions after applying the complete selection to the resonant channel

7 Mass Fits

7.1 Resonant Channel

To obtain the number of signal events we fit the B_s mass with a Double Crystal Ball function where both Crystal Balls share the same parameters for the mean, α and n. Only the standard deviation may vary between the two Crystal Balls. The fit can be seen in figures 14a and 14b (logarithmic scale).

Moreover, a fit is done for the combined dikaon mass. As the f_2' resonance is relatively broad, the shape of the peak is not dominated by the detector resolution and it can therefore be fit with the Breit Wigner function. The fit is shown in figure 15.

The problem is, that the peak in the B_s mass also contains the decay $B_s \to K^+K^-\mu^+\mu^-$ where the two kaons do not come from the f_2' resonance. To distinguish between this decay and the decay $B_s \to f_2' J/\psi$ we do a two dimensional massfit of the combined B_s and dikaon mass. The two dimensional histogram for the resonant channel can be seen in figure 16.

We fit this distribution with the following probability density function (pdf) in the two variables m_B and m_{KK}:

$$\begin{aligned} \mathcal{P}_{tot}(m_B, m_{KK}; \vec{\lambda}) &= N_R \cdot S_R + N_{NR} \cdot S_{NR} + N_B \cdot B \qquad \text{with} \\ S_R &= DCB(m_B; \vec{\lambda}) \cdot BW(m_{KK}; \vec{\lambda}) \,, \\ S_{NR} &= DCB(m_B; \vec{\lambda}) \cdot Exp(m_{KK}; \vec{\lambda}) \,, \\ B &= Exp(m_B; \vec{\lambda}) \cdot Exp(m_{KK}; \vec{\lambda}) \,. \end{aligned}$$

In this context the index R stands for the resonant component (that means decaying through the intermediate state f_2') and NR for the non-resonant (in terms of f_2') component where the B_s meson directly decays into two kaons. Both the resonant and the non-resonant component will be fit the same Double Crystal Ball (DCB) function (see again 14a) in the B_s mass but their Pdfs differ in the dikaon mass: There the resonant component will be again fit with a Breit Wigner function (BW) (see again 15) and the non-resonant component with an exponential function. The combinatorial background B is fit with two different exponential functions in the two variables. The fit is done as an extended fit, so that also the total number of events is part of the fitparameters $\vec{\lambda}$. The fit results can be regarded in figures 17a and 17b. The resulting number of events for the three components are shown in table 6.

7.2 Non-resonant Channel

A similar procedure is done for the non-resonant channel. The two dimensional histogram for this channel can be seen in figure 18.

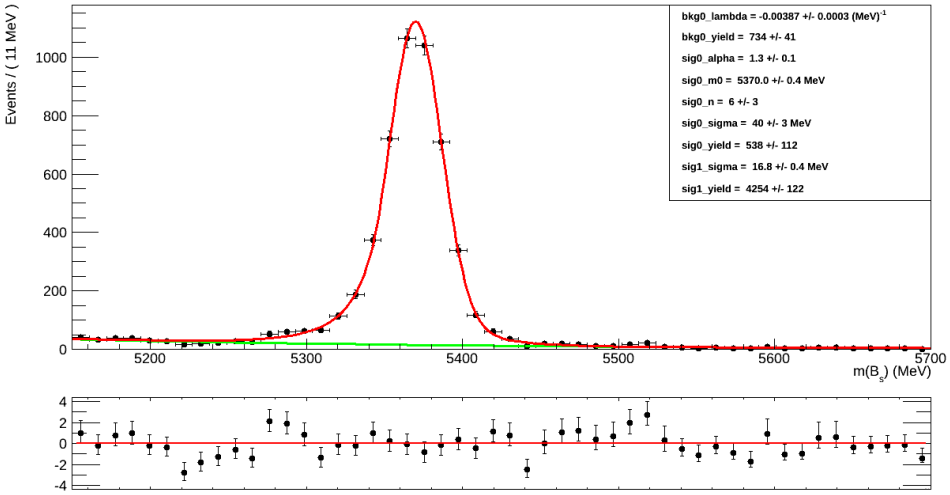

(a) Non-logarithmic scale

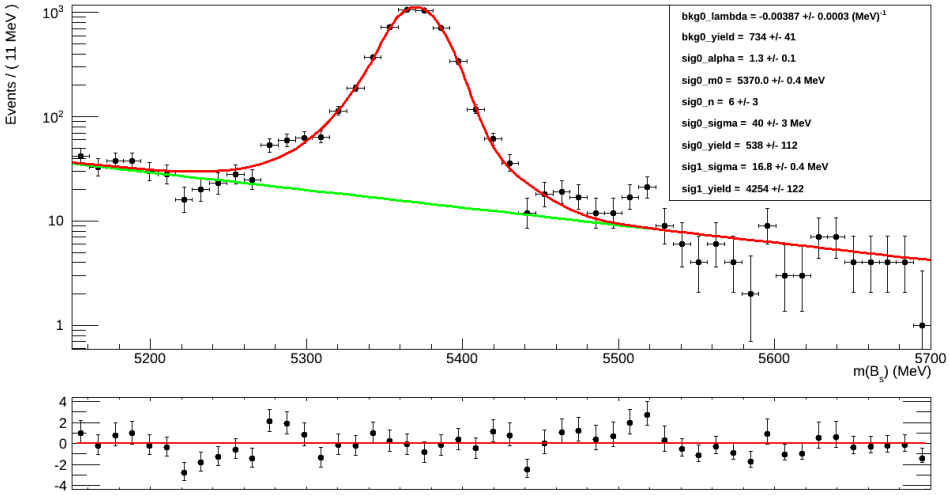

(b) Logarithmic scale

Abb. 14: Fit of the combined B_s mass after the complete selection for the resonant channel

Tab. 6: 2D-fit results: Yields for the resonant channel in the different components

Component	Yield
$B_s \to f_2' J/\psi$	1892.17 ± 80.47
$B_s \to K^+K^- J/\psi$	2929.93 ± 90.18
Combinatorial BKG	703.94 ± 45.79

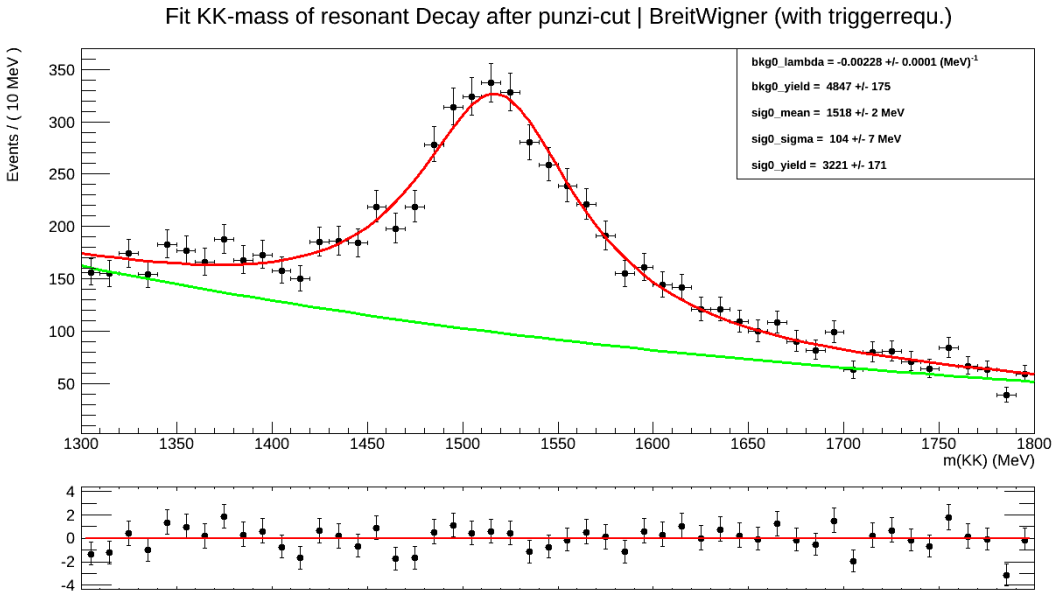

Abb. 15: Fit of the combined dikaon mass after the complete selection for the resonant channel

Tab. 7: 2D-fit results: Yields for the rare decay in the different components

Component	Yield
$B_s \to f_2'\mu^+\mu^-$	17.21 ± 2.86
$B_s \to K^+K^-\mu^+\mu^-$	26.65 ± 4.43
Combinatorial BKG	22.13 ± 5.63

We fit this distribution with the same pdf as for the resonant channel, where we fix the parameters for both signal components and moreover the ratio between the f_2' resonant and KK non-resonant component, where we take the values from the fit of the normalisation channel. This is necessary as we do not have enough events in the non-resonant channel to leave them variable. The fit results for the non-resonant channel can be regarded in the figures 19a and 19b. The resulting yields are shown in table 7. That means we observe 17.21 ± 2.86 signal events for the rare decay $B_s \to f_2'\mu^+\mu^-$.

8 Efficiencies

The efficiencies are calculated using simulated events. As we only have the simulation for $B_s \to f_2'\mu^+\mu^-$ a cut of $\pm 50\,\mathrm{MeV}$ around the nominal J/ψ mass is applied to also calculate the efficiencies for the normalisation channel $B_s \to f_2'J/\psi$. As this results in less events to be considered, the statistical errors for this decay will in general be higher than the efficiencies for the non-resonant decay where we can use the complete (truthmatched)

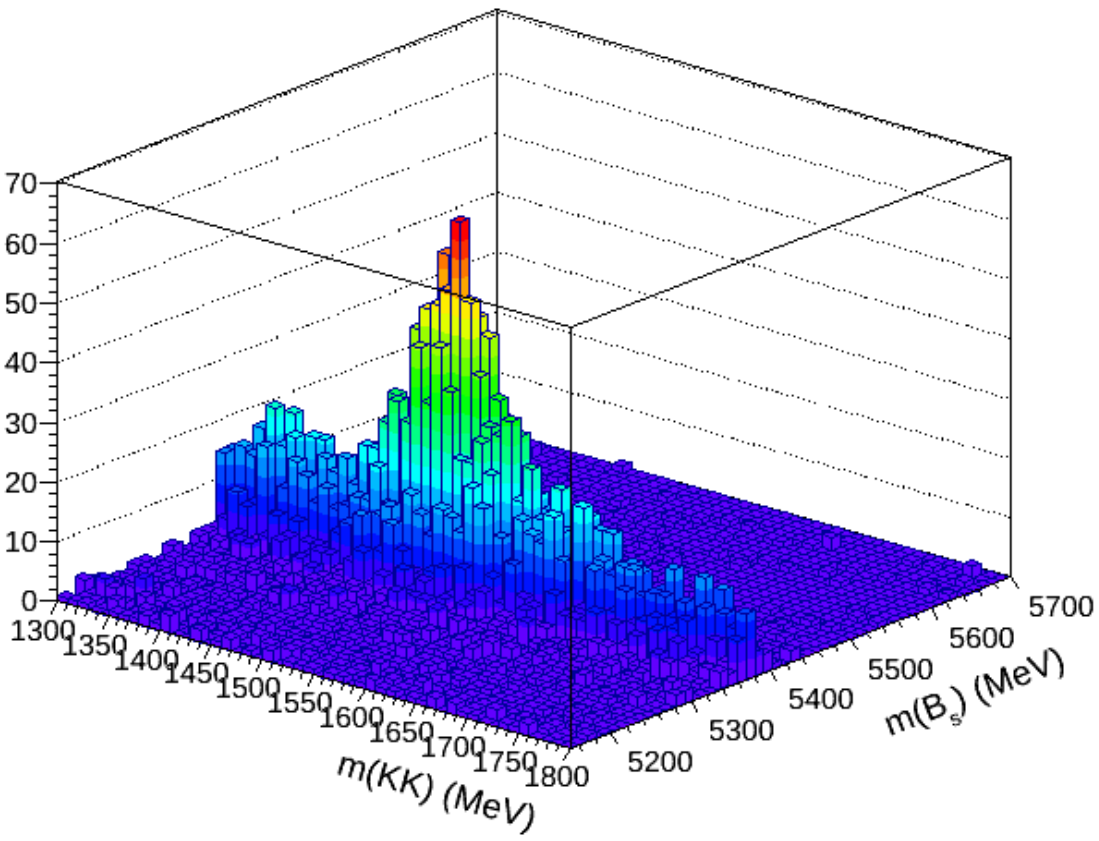

Abb. 16: Two dimensional mass distribution of B_s and dikaon mass for the resonant channel

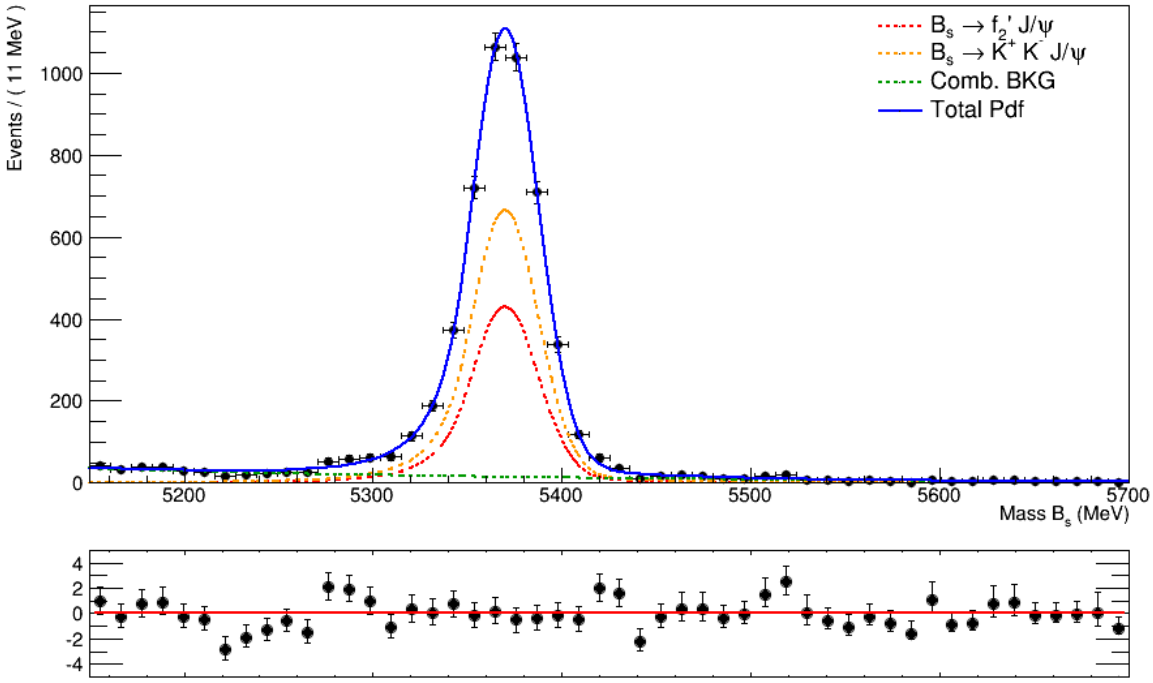

(a) Projection on B_s mass

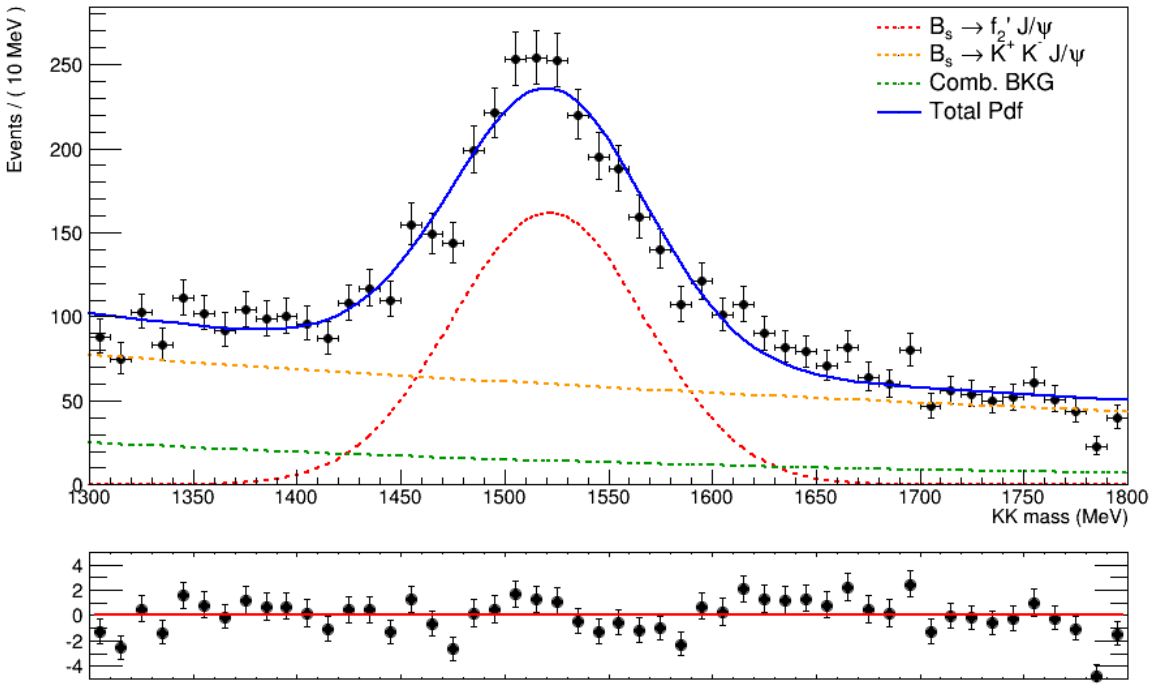

(b) Projection on KK mass

Abb. 17: Fit results of the two dimensional fit of the resonant decay $B_s \to f_2' J/\psi$

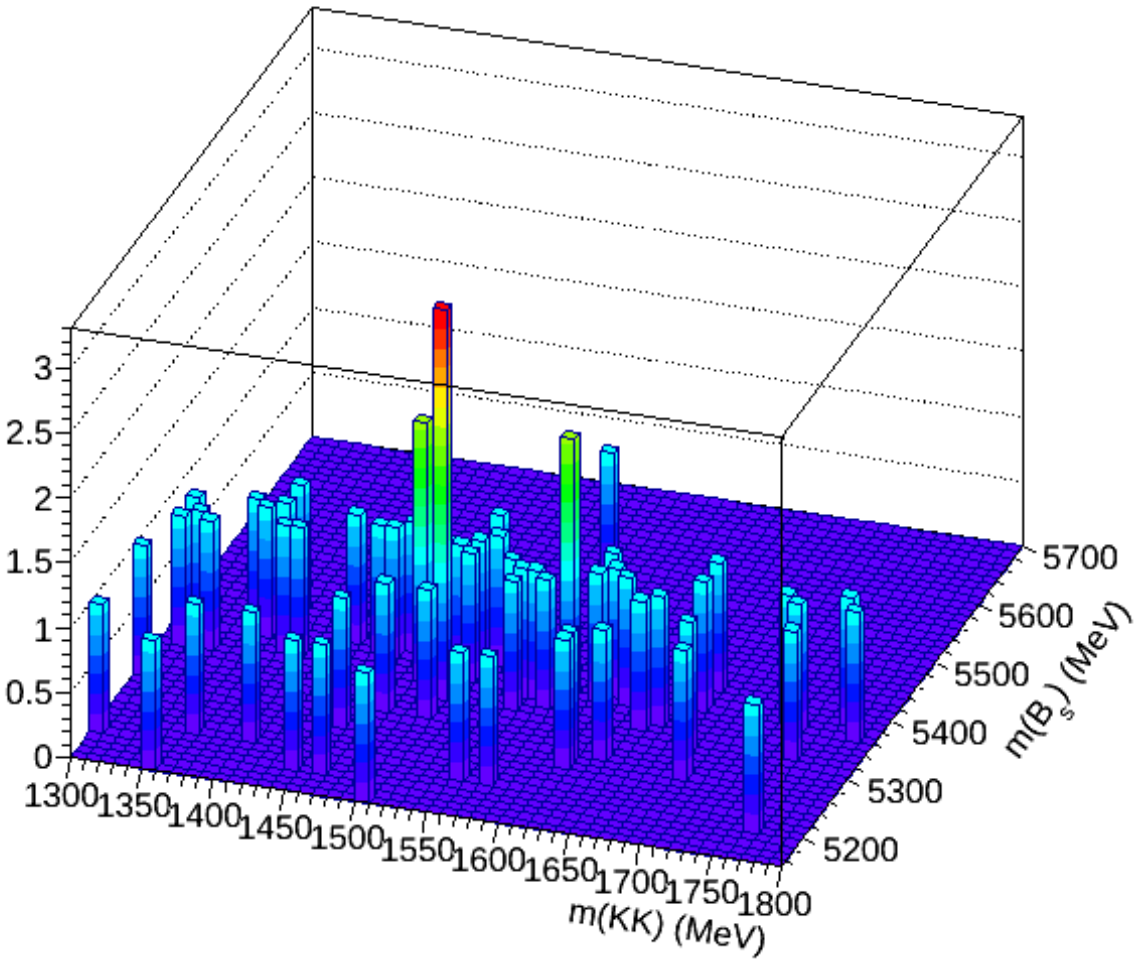

Abb. 18: Two dimensional mass distribution of B_s and dikaon mass for the non-resonant channel

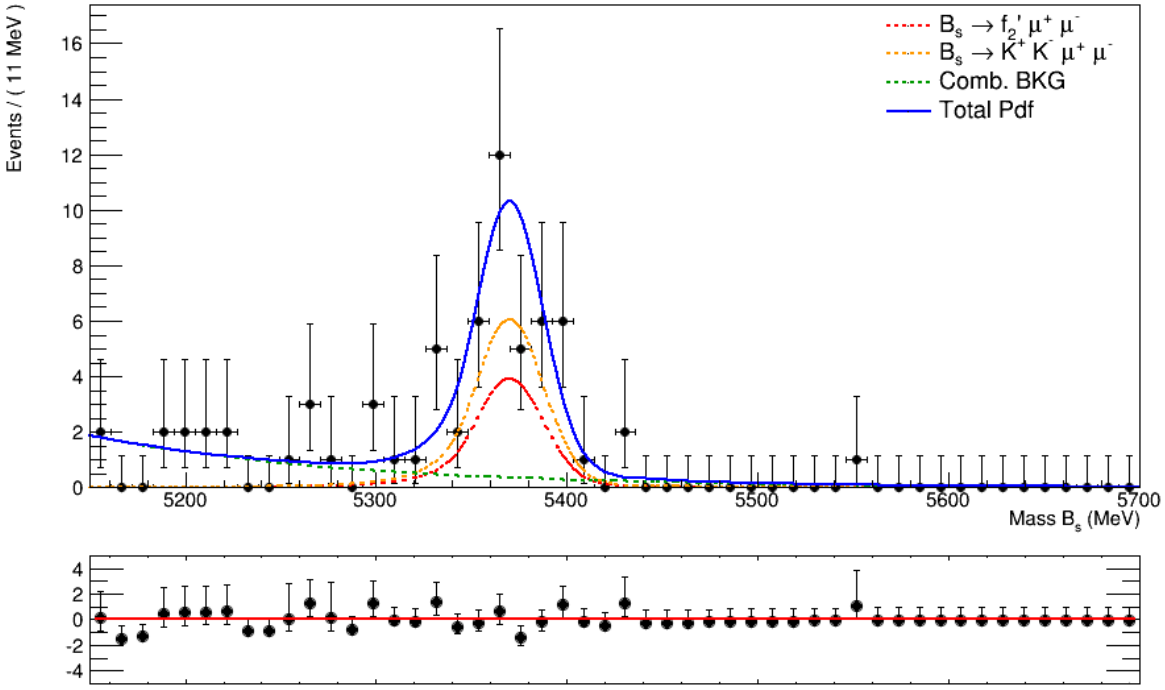

(a) Projection on B_s mass

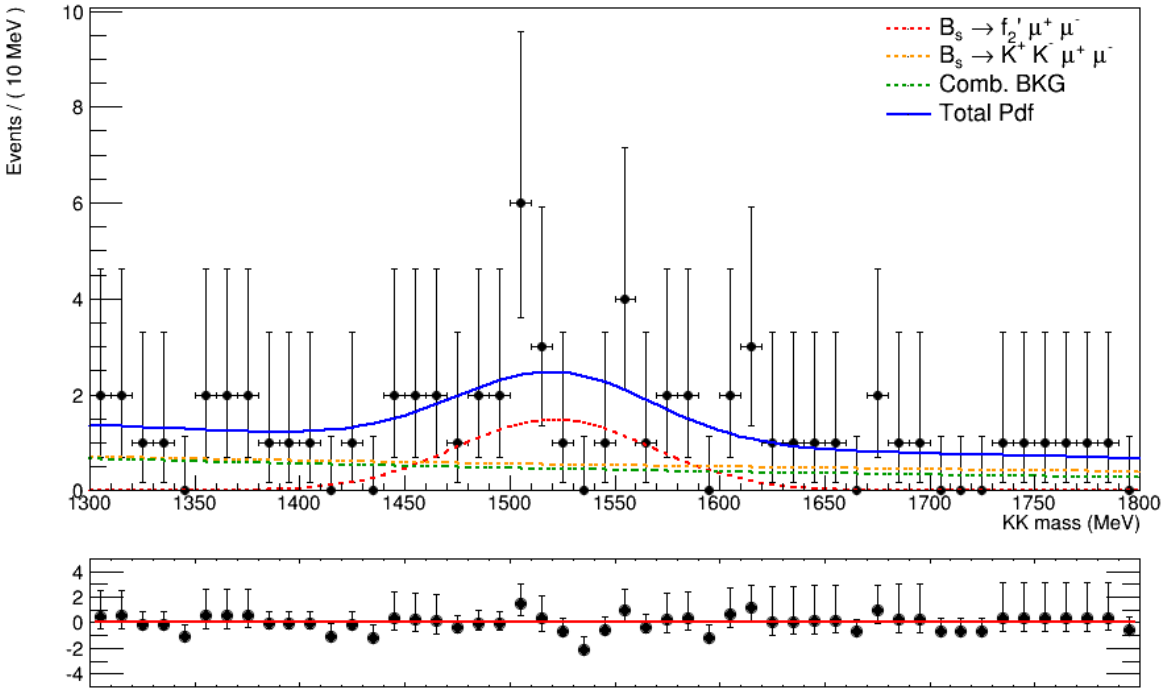

(b) Projection on KK mass

Abb. 19: Fit results of the two dimensional fit of the resonant decay $B_s \to f_2' J/\psi$

Tab. 8: Efficiencies calculated from simulated events

Efficiency	$B_s \to f_2' J/\psi$ [%]	$B_s \to f_2' \mu^+\mu^-$ [%]
ϵ_{gen}	17.171 ± 0.684	16.496 ± 0.049
$\epsilon_{\text{rec,strip\|gen}}$	10.5801 ± 0.0877	10.1046 ± 0.0161
$\epsilon_{\text{presel\|rec,strip}}$	72.0642 ± 0.3933	56.9499 ± 0.0831
$\epsilon_{\text{BDT\|presel}}$	37.0054 ± 0.4986	40.1327 ± 0.1091
$\epsilon_{\text{trig\|BDT}}$	87.8963 ± 0.5537	73.8979 ± 0.1542
ϵ_{tot}	0.4258 ± 0.0186	0.2815 ± 0.0014

Monte Carlo sample. Moreover, a generator cut level efficiency for the resonant decay could not be found in the Table for Generation [4] which made it necessary to calculate it ourselves with a simple simulation. The generator level cut efficiency for the non-resonant channel was calculated to be $\epsilon_{\text{gen,res}} = (17.171 \pm 0.684)\,\%$. The generator level cut efficiency for the rare decay $B_s \to f_2'\mu^+\mu^-$ was taken from the MC Generation table to be $\epsilon_{\text{gen,non-res}} = (16.496 \pm 0.049)\,\%$.

The remaining efficiencies can be found in table 8.

Note that the preselection efficiencies here also include the cuts on the dimuon mass for the particular channel as given in table 5. The total efficiencies are calculated as the product of ϵ_{gen} and the ratio of events passing the complete selection to events in the MCDecayTree. This results in lower statistical errors than multiplying the single efficiencies as given in table 8.

9 Peaking Backgrounds

We have evidence, that there are still several background events coming from misidentified particles. Therefore the decays $B \to J/\psi K^*(\to K\pi)$, $B \to \mu^+\mu^- K^*(\to K\pi)$ and $\Lambda_b \to \mu^+\mu^-\Lambda(1520)(\to Kp)$, where the proton/pion is misidentified as a kaon, were considered. We use simulations to calculate the efficiencies for these decays. With help of the normalisation channel and the branching ratios of these decays [2] we can get an estimate for the number of events belonging to these misidentified decays that end up in our mass windows we use for the fitting.

9.1 $B \to J/\psi K^*(\to K\pi)$

Figure 20 shows the two dimensional distribution in the B_s and KK mass after applying the complete selection to the simulation of this decay. Note that the total number of

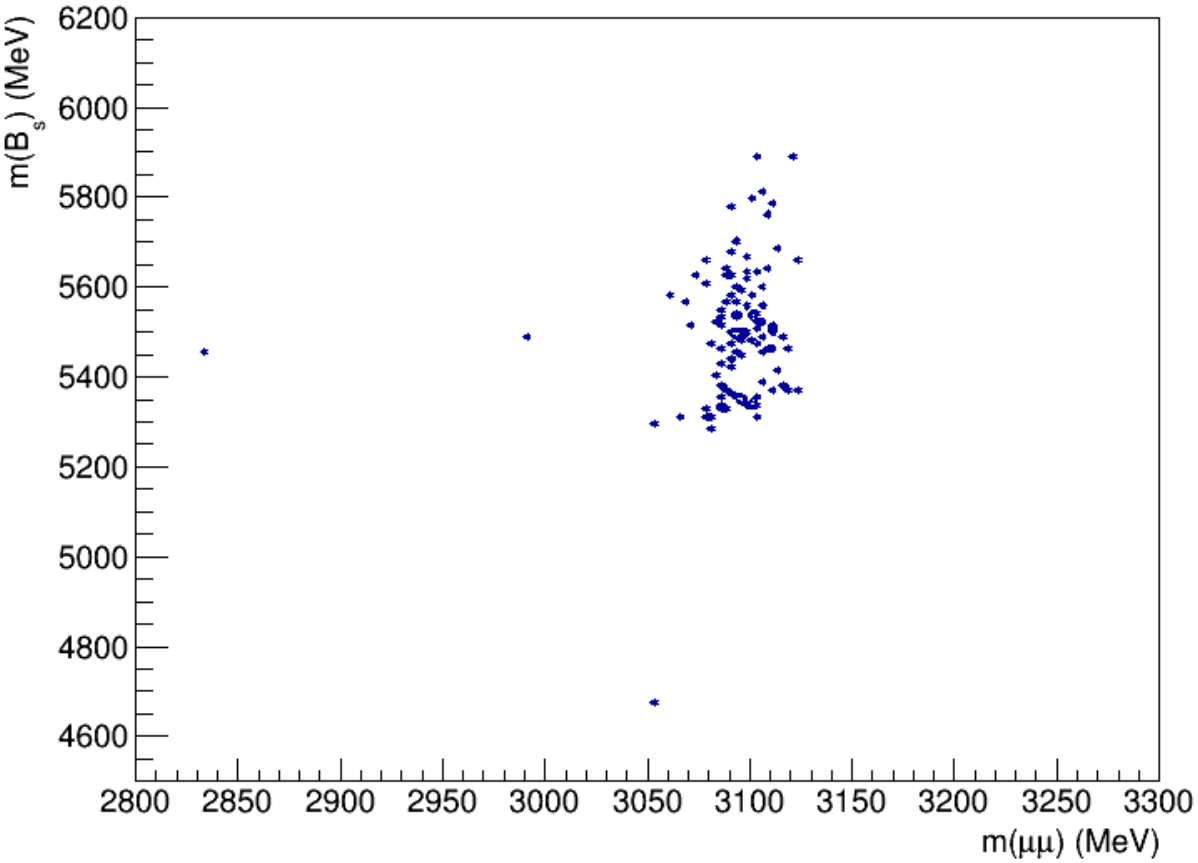

Abb. 20: Two dimensional mass distribution of B_s and dikaon mass for the simulation of $B \to J/\psi K^*(\to K\pi)$ after the selection

events ending up there is only determined by the size of the simulation sample and the efficiency of the selection. It does not represent the actual events ending up there in the data. To get an estimate for the actual events ending up in our mass windows the formula

$$N(\text{peaking}) = \frac{N_{\text{res}}}{\mathcal{B}(\text{res}) \cdot \epsilon_{\text{res}}} \cdot \frac{f_d}{f_s} \cdot \mathcal{B}(\text{peaking}) \cdot \epsilon_{\text{peaking}} \tag{4}$$

$$= N(B_s \text{ produced}) \cdot \frac{f_d}{f_s} \cdot \mathcal{B}(\text{peaking}) \cdot \epsilon_{\text{peaking}} \tag{5}$$

$$= N(B_d \text{ produced}) \cdot \mathcal{B}(\text{peaking}) \cdot \epsilon_{\text{peaking}} \tag{6}$$

with the resonant/normalisation channel $B_s \to f_2' J/\psi$ where $f_2' \to K^+K^-$ and the ratio of produced B_d and B_s mesons $\frac{f_d}{f_s}$ is used.

From the normalisation channel we obtain $N_{\text{res}} = 1892.17 \pm 80.47$ and $\epsilon_{\text{res}} = (0.426 \pm 0.019)\,\%$.

The branching ratio of the normalisation channel is calculated to be

$$\mathcal{B}(\text{res}) = \mathcal{B}(B_s \to f_2' J/\psi) \cdot \mathcal{B}(f_2' \to K^+K^-) \cdot \mathcal{B}(J/\psi \to \mu^+\mu^-) = (6.84 \pm 1.59) \cdot 10^{-6}$$

with

$\mathcal{B}(B_s \to f_2' J/\psi) = (2.6 \pm 0.6) \cdot 10^{-4}$,
$\mathcal{B}(f_2' \to K^+K^-) = (44.4 \pm 1.1)\,\%$,
$\mathcal{B}J/\psi \to \mu^+\mu^- = (5.961 \pm 0.033)\,\%$.

The branching fractions were taken from the PDG [2], where the value for $\mathcal{B}(f_2' \to K^+K^-)$ was taken to be the half of $\mathcal{B}(f_2' \to \overline{K}K)$ [1]. The value of $\frac{f_d}{f_s} = 3.86 \pm 0.22$ was calculated from the value of $\frac{f_s}{f_d}$ taken from [5].

The branching ratio for $B \to J/\psi K^*$ is composited from

$$\mathcal{B}(\text{peaking}) = \mathcal{B}(B \to J/\psi K^*) \cdot \mathcal{B}(J/\psi \to \mu^+\mu^-) \cdot \mathcal{B}(K^* \to K^{+/-}\pi^{+/-}) = (3.93 \pm 0.18) \cdot 10^{-6}$$

with

$\mathcal{B}(B \to J/\psi K^*) = (1.32 \pm 0.06) \cdot 10^{-3}$,
$\mathcal{B}(J/\psi \to \mu^+\mu^-) = (5.961 \pm 0.033)\,\%$,
$\mathcal{B}(K^* \to K^{+/-}\pi^{+/-}) \approx 50\,\%$

where $\mathcal{B}(K^* \to K^{+/-}\pi^{+/-})$ is taken to be the half of $\mathcal{B}(K^* \to K\pi)$ [2].

The efficiency of the peaking background for the resonant channel (that means choosing only events with a dimuon mass in the range of $\pm 50\,\text{MeV}$ around the nominal J/ψ mass) is, using the simulation, calculated to be $\epsilon_{\text{peaking,res}} = (7.55 \pm 0.77) \cdot 10^{-6}$. This efficiency now also includes a cut on the B_s mass to be in the used fit range of $5150\,\text{MeV/c}^2 < m(B_s) < 5700\,\text{MeV/c}^2$. This results in a number of misidentified events coming from this decay and ending up in the resonant fit windows of $N(\text{peaking,res}) = 74 \pm 20$.

For the non-resonant channel (that means excluding the charmonium resonances) the efficiency (including the cut on the B_s mass) is calculated to be $\epsilon_{\text{peaking,non-res}} = (3.97 \pm 1.77) \cdot 10^{-7}$ resulting in $N(\text{peaking,non-res}) = 3.9 \pm 2.0$ events in the fit windows - which is compared to the number of obtained rare decay events of 17.21 ± 2.86 a non-negligible contribution.

9.2 $B \to \mu^+\mu^- K^*(\to K\pi)$

Figure 21 shows again the two dimensional distribution in the B_s and KK mass after applying the complete selection to the simulation of this decay.

The branching ratio for this decay is composited of

$$\mathcal{B}(\text{peaking}) = \mathcal{B}(B \to \mu^+\mu^- K^*) \cdot \mathcal{B}(K^* \to K^{+/-}\pi^{+/-}) = (5.52 \pm 0.50) \cdot 10^{-7}$$

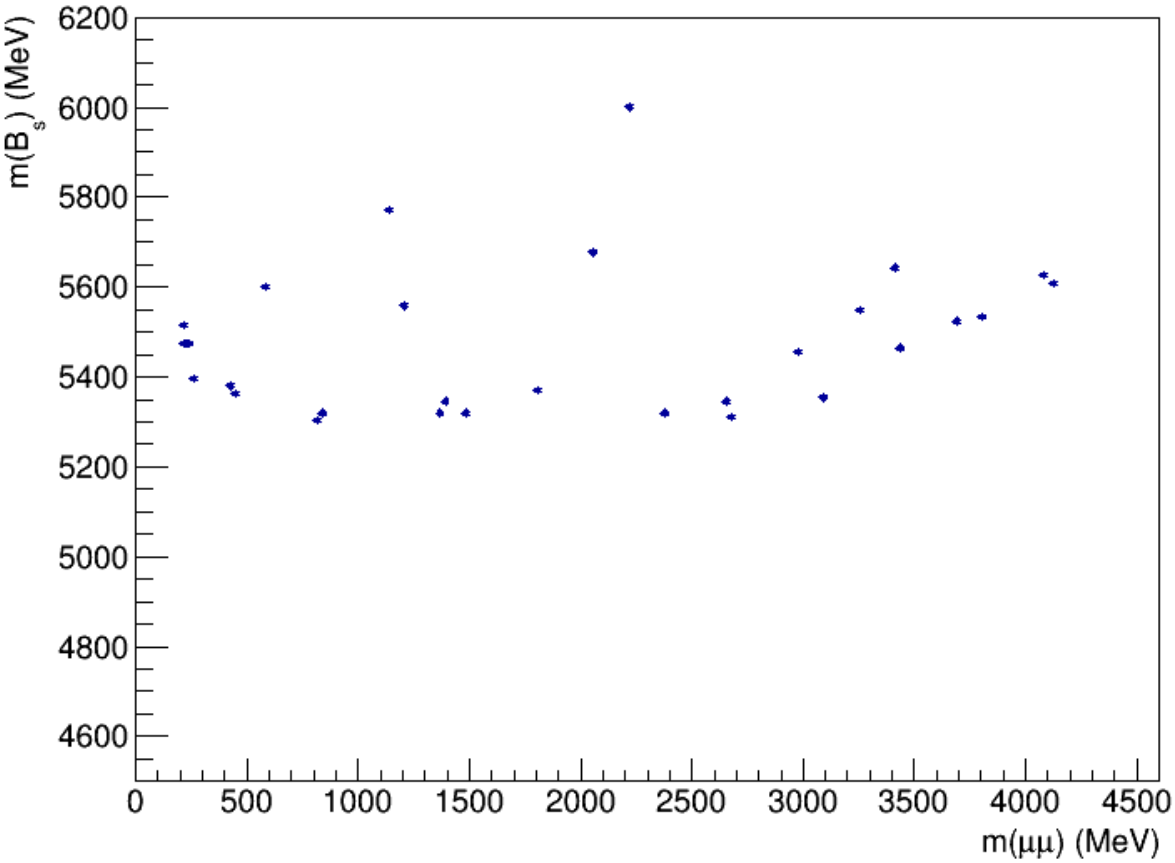

Abb. 21: Two dimensional mass distribution of B_s and dikaon mass for the simulation of $B \to \mu^+\mu^- K^*(\to K\pi)$ after the selection

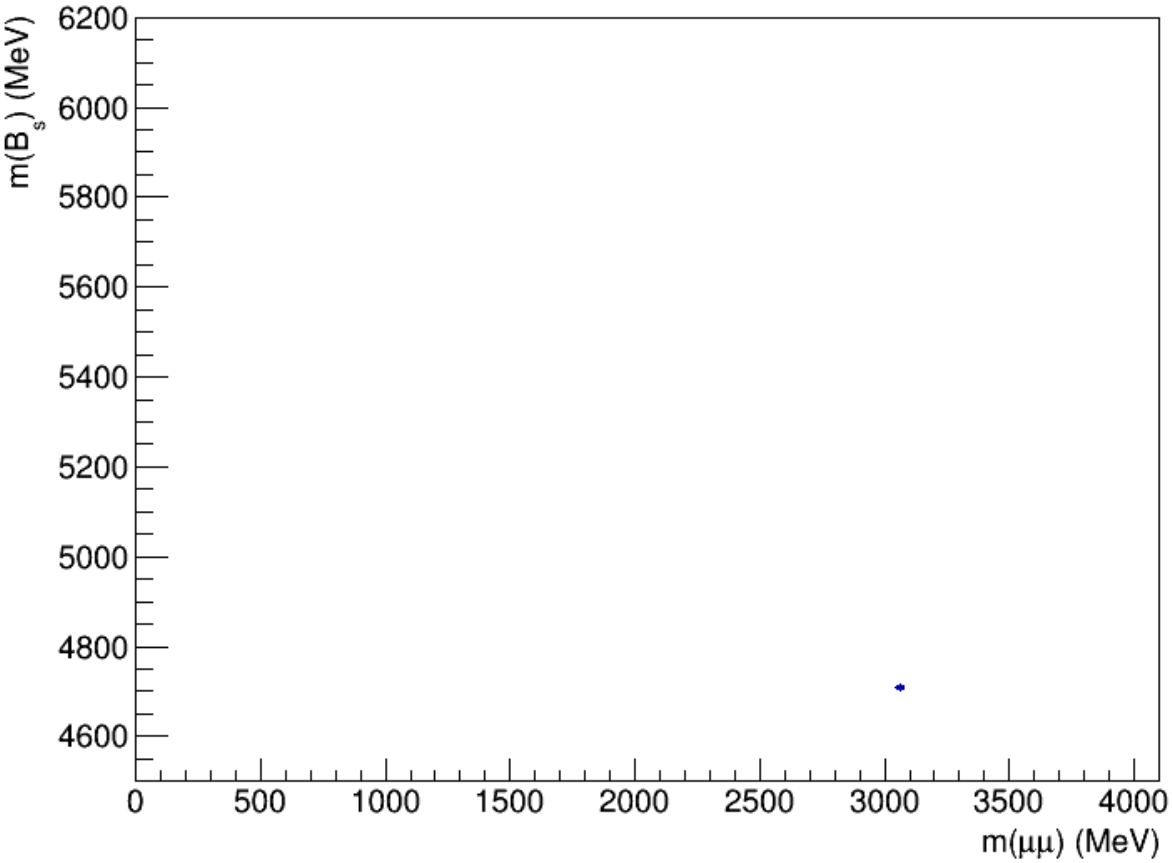

Abb. 22: Two dimensional mass distribution of B_s and dikaon mass for the simulation of $\Lambda_b \to \mu^+\mu^-\Lambda(1520)(\to Kp)$ after the selection

and the efficiencies could be calculated to be $\epsilon_{\text{peaking,res}} = (3.98 \pm 3.98) \cdot 10^{-7}$ for the resonant and $\epsilon_{\text{peaking,non-res}} = (8.75 \pm 1.87) \cdot 10^{-6}$ non-resonant channel. The large errors on these numbers result in a small Monte Carlo sample. This results in $N(\text{peaking,res}) = 0.05 \pm 0.05$ events in the resonant fit windows and $N(\text{peaking,res}) = 1.15 \pm 0.39$ in the non-resonant fit windows. That means it is negligible for the resonant fit but has to be taken into account when fitting the rare decay.

9.3 $\Lambda_b \to \mu^+\mu^-\Lambda(1520)(\to Kp)$

Figure 22 shows again the two dimensional distribution in the B_s and KK mass after applying the complete selection to the simulation of this decay.

Instead of taking $\frac{f_d}{f_s}$ in equation 4 we here have to use the ratio $\frac{f_{\Lambda_b}}{f_s} = 2.31 \pm 0.24$ calculated from $\frac{f_s}{f_u+f_d}$ and $\frac{f_{\Lambda_b}}{f_u+f_d}$ taken from [6].

The branching ratio for this decay is composited of

$$\mathcal{B}(\text{peaking}) = \mathcal{B}(\Lambda_b \to \mu^+\mu^-\Lambda(1520)) \cdot \mathcal{B}(\Lambda(1520) \to Kp) = (2.43 \pm 0.63) \cdot 10^{-7}$$

with

$$\mathcal{B}(\Lambda(1520) \to Kp) = (22.5 \pm 0.5)\,\%$$

where the branching ratio $\mathcal{B}(\Lambda(1520) \to Kp)$ is taken to be the half of $\mathcal{B}(\Lambda(1520) \to N\overline{K})$ [2] as we are only interested in the pK mode. Moreover, the value of $\mathcal{B}(\Lambda_b \to \mu^+\mu^-\Lambda(1520))$ is not known, so we assume it to be the same as $\mathcal{B}(\Lambda_b \to \mu^+\mu^-\Lambda)$.

When calculating the efficiencies including the cut on the B_s mass we end up with 0 events after the selection meaning that we can not calculate the efficiency. That is why we do not include this cut for this peaking background decay, which implies that the actual efficiency will be even smaller than the numbers given below. Moreover, for the non-resonant channel we still end up with 0 events. We therefore assume the same efficiency for both channels.

The efficiencies could then be calculated to be $\epsilon_{\text{peaking}} = (6.65 \pm 6.65) \cdot 10^{-7}$ for both channels. This results in $N(\text{peaking,res}) = 0.024 \pm 0.024$ for each channel which is negligible compared to the total events ending up in our fit windows.

9.4 Conclusion

Especially the decay $B \to J/\psi K^*(\to K\pi)$ has to be taken into account when it comes to fit the mass shapes as it has a non-negligible estimated contribution to the yields. Moreover the decay $B \to \mu^+\mu^- K^*(\to K\pi)$ has to be considered when fitting the non-resonant channel.

10 Comparison of PID Variables in Data and MC

To check if the PID variables in the simulation are a good description of the data, we compare them with help of the normalisation channel. Therefore we look at simulation and data after the preselection. To separate the signal from background in the data we use the sPlot technique [7]. We therefore fit the preselected resonant data (violet area) with a (single) Crystal Ball as signal and an exponential function as background. With every parameter free the fit would not convergate, that is why we fixed the parameter n on simulations. While doing this simple one dimensional fit we will end up with events which are not going through the intermediate resonance f_2' but where the B_s decays in two kaons directly. We assume here that these decays do not differ too much when

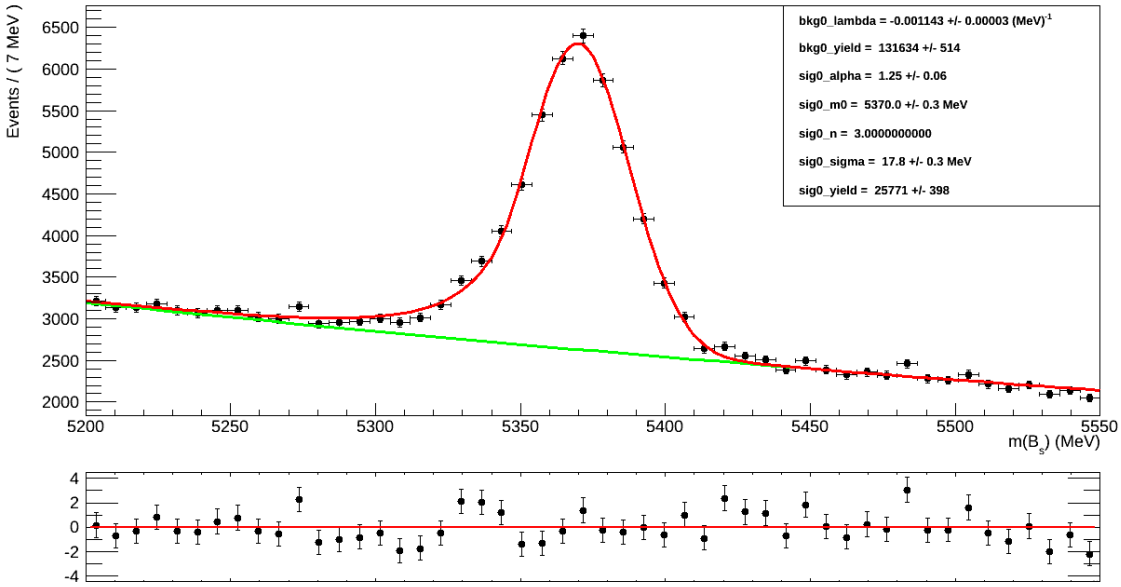

Abb. 23: Fit of the $B_s \to f_2' J/\psi$ after the preselection with a Crystal Ball to get sWeights

looking at the PID variables in the given KK mass from 1300 MeV/c^2 to 1800 MeV/c^2. The fit can be seen in figure 23.

The sWeights getting from this fit are used to compare the data with the simulation. The (normalised) comparison histograms can be seen in the figures 24-26.

Especially in the Kaon PID distributions you can see a significant shift resulting in non-optimal BDT training and systematic biases in the efficiency calculation.

Literatur

[1] **The LHCb Collaboration**, R. e. a. Aaij, „Observation of $\overline{B}{}^0_s \to J/\psi f_2'(1525)$ in $J/\psi K^+K^-$ Final States“. *Phys. Rev. Lett.* **108** (Apr, 2012) 151801.

[2] **Particle Data Group**, J. Beringer *et al.*, „Review of Particle Physics“. *Phys. Rev. D* **86** (Jul, 2012) 010001.

[3] G. Punzi, „Sensitivity of searches for new signals and its optimization“. *eConf* **C030908** (2003) MODT002, `arXiv:physics/0308063 [physics]`.

[4] LHCb, „Table for Generation“. `http://lhcb-release-area.web.cern.ch/LHCb-release-area/DOC/STATISTICS/SIM08STAT/RD-WG/Generation_Sim08-Beam4000GeV-mu100-2012-nu2.5-Pythia8.html`. Visited 2014-09-17.

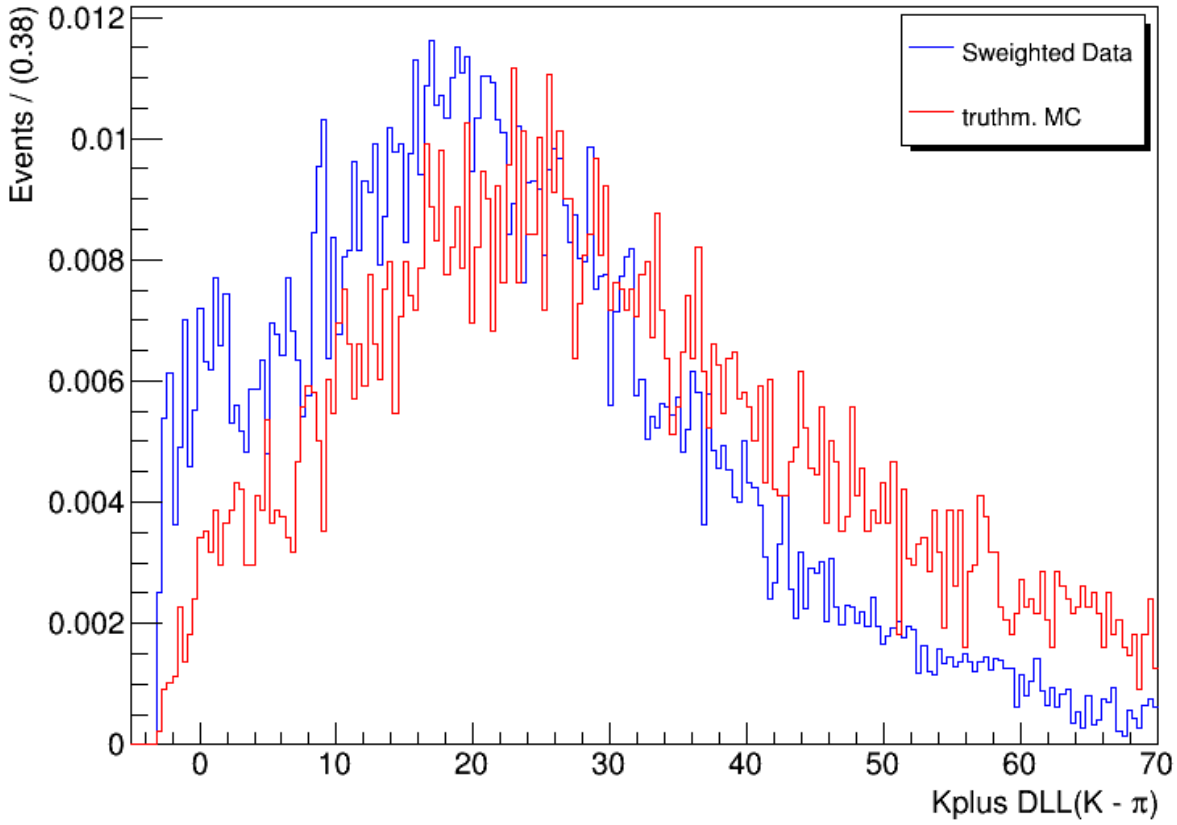

Abb. 24: Comparison of sWeighted data to simulation for the resonant channel $B_s \to f_2' J/\psi$ - Kaon DLL($K - \pi$)

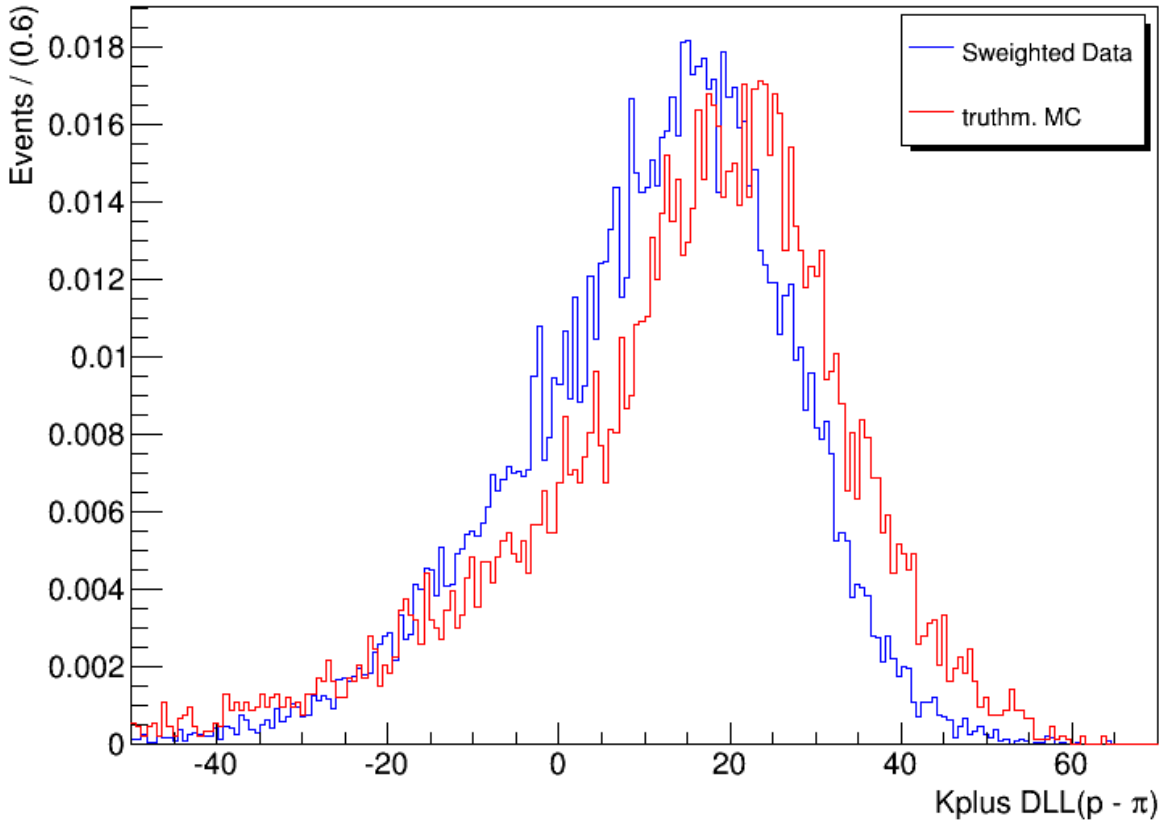

Abb. 25: Comparison of sWeighted data to simulation for the resonant channel $B_s \to f_2' J/\psi$- Kaon DLL$(p - \pi)$

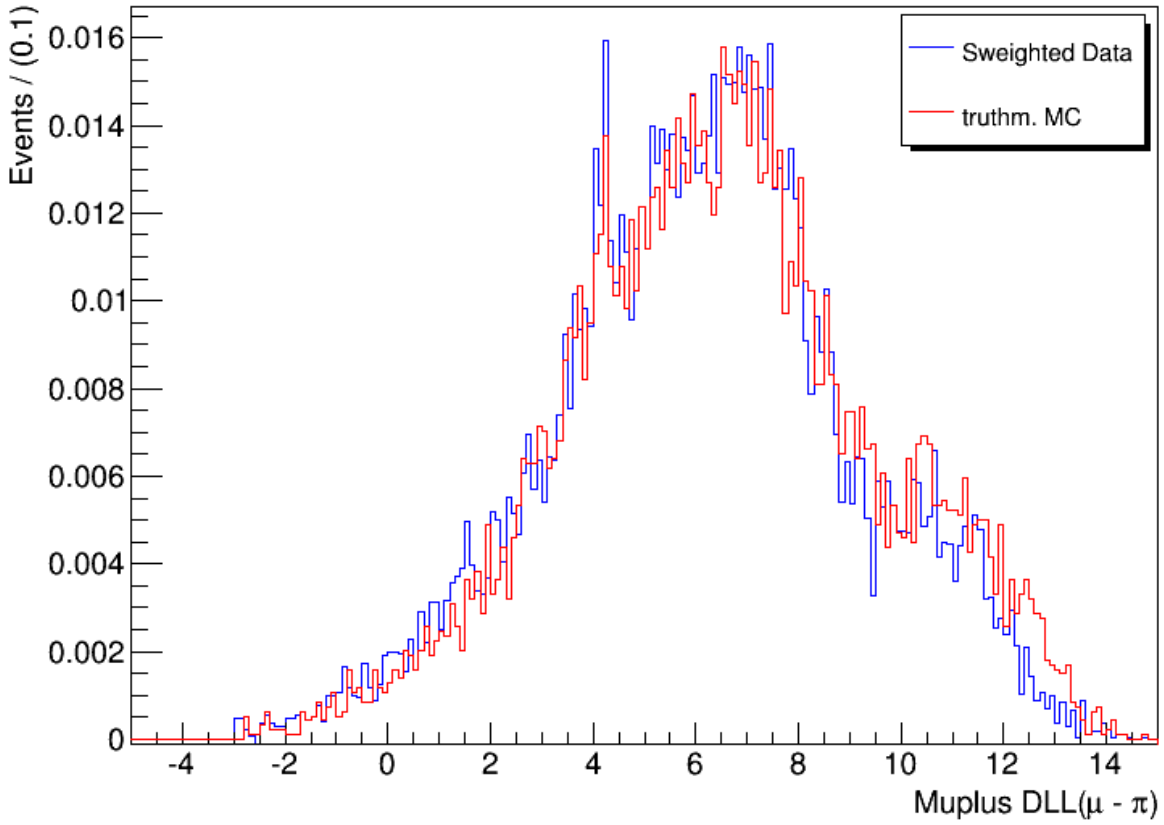

Abb. 26: Comparison of sWeighted data to simulation for the resonant channel $B_s \to f_2' J/\psi$ - Muon DLL($\mu - \pi$)

[5] **LHCb Collaboration**, „Updated average f_s/f_d b-hadron production fraction ratio for 7 TeV pp collisions“.

[6] **Heavy Flavor Averaging Group**, Y. Amhis *et al.*, „Averages of B-Hadron, C-Hadron, and tau-lepton properties as of early 2012“. `arXiv:1207.1158 [hep-ex]`.

[7] M. Pivk and F. R. Le Diberder, „sPlot: a statistical tool to unfold data distributions“. *Nucl.Instrum.Meth.* **A555** (2005) 356–369, `arXiv:physics/0402083 [physics.data-an]`.